Teske, A., Lizarralde, D., Höfig, T.W., and the Expedition 385 Scientists
Proceedings of the International Ocean Discovery Program Volume 385
publications.iodp.org

Data report: wavelength dispersive X-ray fluorescence in sediments from all IODP Expedition 385 sites in the Guaymas Basin[1]

Lucie Pastor,[2] Audrey Boissier,[3] and Céline Burin[4]

[1] Pastor, L., Boissier, A., and Burin, C., 2023. Data report: wavelength dispersive X-ray fluorescence in sediments from all IODP Expedition 385 sites in the Guaymas Basin. In Teske, A., Lizarralde, D., Höfig, T.W., and the Expedition 385 Scientists, Guaymas Basin Tectonics and Biosphere. Proceedings of the International Ocean Discovery Program, 385: College Station, TX (International Ocean Discovery Program). https://doi.org/10.14379/iodp.proc.385.203.2023
[2] University of Brest, CNRS, IFREMER, France. Correspondence author: **luciepastor@yahoo.fr**
[3] Geo-Ocean CNRS-IFREMER-UBO-UBS, France.
[4] Department of Earth & Ocean Sciences, School of Natural Sciences, National University of Ireland, Ireland.

Contents

Keywords
International Ocean Discovery Program, *JOIDES Resolution*, Expedition 385, Guaymas Basin Tectonics and Biosphere, Site U1545, Site U1546, Site U1547, Site U1548, Site U1549, Site U1550, Site U1551, Site U1552, X-ray fluorescence, XRF

References (RIS)

MS 385-203
Received 21 February 2023
Accepted 30 March 2023
Published 14 June 2023

Abstract

International Ocean Discovery Program (IODP) Expedition 385 focused on the impact of sill emplacement and fluid flow on subsurface biogeochemical processes in organic-rich sediments of the Guaymas Basin. It resulted in the drilling of eight sites with contrasted settings; Sites U1545 and U1546 were drilled in the northern basin and allowed the recovery of a deep sill at Site U1546; Sites U1547 and U1548 were drilled on an active hydrothermal vent called Ringvent; Sites U1549 and U1552 were drilled on the Sonora margin where cold seeps and hydrates were identified; Site U1550 was sampled as a replicate of Deep Sea Drilling Project (DSDP) Leg 64 Site 481 on an axial trough; and Site U1551 was drilled ~29 km southeast of the axial graben and was mainly terrigenous. The quantitative X-ray fluorescence data presented here were measured on squeeze cakes retrieved after squeezing of whole-round core segments for pore water extraction. Major elements (Al, Ca, Cl, Fe, K, Mg, Mn, Na, P, Si, Ti, and S) as well as minor/trace elements (As, Ba, Br, Ce, Co, Cr, Cu, La, Mo, Nb, Ni, Pb, Rb, Sc, Sr, V, Y, Zn, and Zr) are provided in this data report.

1. Introduction

The Guaymas Basin, located in the Gulf of California, is a young marginal rift basin with active seafloor spreading (Calvert, 1966). It is a unique feature where hydrothermal vents (mainly in the southern trough) and cold seeps (Sonora margin) are only separated by 60 km without any physical barrier and where the seafloor is covered by several hundred meters of organic-rich sediments (2–4 wt% organic carbon). Newly formed crust at the spreading axis intrudes into the overlying sediments as sills and dikes (Einsele et al., 1980). In the hydrothermal area, this process is responsible for complex subsurface circulation patterns, with thermogenic alteration of sediments leading to the production of fluids that differ from other more conventional hydrothermal sites (e.g., more enriched in methane and sulfides) (Von Damm et al., 1985; Sturz et al., 1996). Field programs conducted in the Guaymas Basin, including Deep Sea Drilling Project (DSDP) Leg 64, have provided the framework for a better understanding of thermal alterations of sedimentary organic matter and the chemical composition of hydrothermal fluids. During International Ocean Discovery Program (IODP) Expedition 385, eight sites were drilled in the Guaymas Basin with the aim of unraveling the impact of sill intrusion on physical, chemical, and biological processes in organic-rich sediments.

The geochemical characterization of these hemipelagic sediments using quantitative X-ray fluorescence are provided in this report as a starting point for discussing sediment sources, sedimentological features, and geochemical alteration.

2. Study sites

Eight sites were investigated during Expedition 385 in the Guaymas Basin (Figure **F1**). Detailed background and objectives are given in **Teske et al.** (2021b). The main objective was to elucidate the impact of sill intrusions in different settings. Briefly, Sites U1545 and U1546 are located ~52 km northwest of the axial graben of the northern Guaymas Basin spreading segment. Because these two sites are only 1.1 km apart with a sill intrusion at Site U1546, their comparison enables the quantification of thermal and hydrothermal alteration linked to the sill intrusion. Sites U1547 and U1548 are located ~27 km northwest of the axial graben of the northern Guaymas Basin. They were drilled inside (Holes U1457A–U1457E), at the periphery (Holes U1548A–U1548C), and 600 m west-northwest (Holes U1548D and U1548E) of a circular, bowl-shaped active hydrothermal mound called Ringvent. The intrusion of a sill at shallow depths induced a very steep heat flow, as well as hot fluid circulation (Teske et al., 2019). Sites U1549 and U1552 are located, respectively, 9.5 and 20 km northwest of the northern axial graben in the Guaymas Basin, proximal to the Sonora margin. In this location, a deep sill, the presence of surficial gas hydrates, and visible cold-seep communities drive a multicomponent study of the carbon cycle. Site U1550 was drilled at the same position as DSDP Leg 64 Site 481 within the axial graben of the northern Guaymas Basin spreading segment. The objective was to better recover the sill at this site and thus to better characterize its impact on the surrounding sediment. Finally, Site U1551 is located ~29 km southeast of the axial graben of the northern Guaymas Basin spreading segment. At this site, the sediment source is mainly terrestrial and may be impacted differently by the presence of a deep sill.

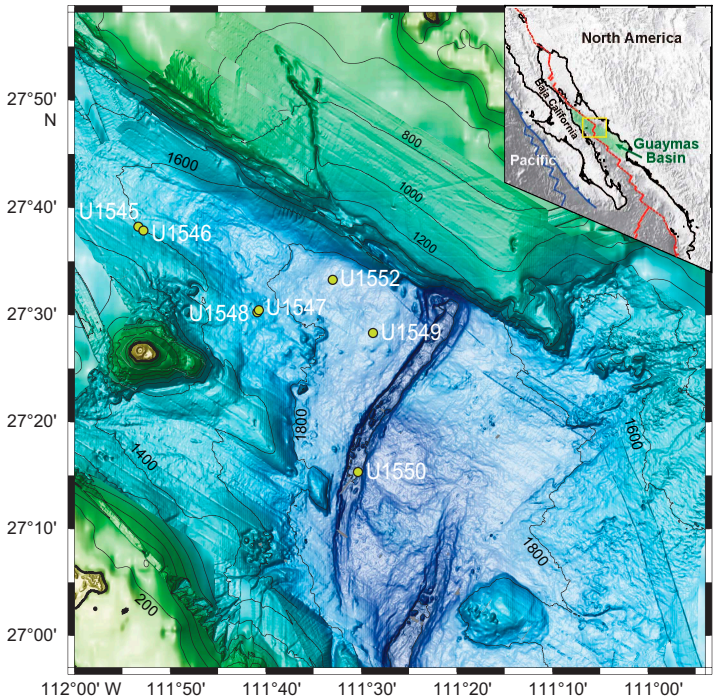

Figure F1. Study area and sample locations, Expedition 385. Modified from Teske et al. (2021b).

Table T1. Analytical details for each element, Expedition 385. **Download table in CSV format.**

3. Methods

After pore water extraction on the R/V *JOIDES Resolution* from ~5–20 cm whole-round segments on average (**Teske et al.**, 2021a), the remaining sediment (squeeze cake) was dispatched and one subportion was enclosed in a vacuumed bag and frozen at –20°C for further analyses, including X-ray fluorescence (XRF).

In the laboratory onshore, sediment was freeze-dried and manually crushed into a fine powder using an agate mortar. Mechanical grinding with an agate mortar was used for samples containing higher amounts of sand (e.g., Site U1551). Sediment quantitative chemical data were acquired using XRF at the Department of Marine Geosciences at IFREMER (Plouzané, France). Analyses were conducted using a wavelength dispersive XRF spectrometer (WDXRF; Bruker AXS S8 TIGER) on fusion beads or pressed pellets for major and trace or volatile elements, respectively. Fusion beads were prepared as follows: 0.5 g of calcined sample (1 h and 40 min at 1050°C) was placed in a Pt-Au crucible with 9 g of $Li_2B_4O_7$ 90%/LiF 10% (SPCSciences) and 500 µL of a 250 g/L solution of LiBr (Merck). Nonwetting agent was added. The fusion was performed at 1050°C in an electronic furnace. Pressed pellets were prepared with 6 g of sample and 0.6 g of wax, and pressed at 10 T.

Calibration curves were established using certified standard powders from the Centre de Recherches Pétrographiques et Géochimiques (CRPG; i.e., BE-N, IF-G, DT-N, and MA-N), the Canadian Certified Reference Materials Project (CCRMP; 12 standards, e.g., UM-1, UM-2, UM-4, RTS-3a, FER2, etc.), Geo*PT* (17 standards; e.g., HARZ01, ML2, NKT1, etc.), and the Geological Survey of Japan (19 standards; e.g., JB-3, JCFA-1, JLs-1, JSD-2, etc.). These standards were prepared identically and measured during the same runs. After data acquisition, measured net peak intensities corrected from interelement effects were converted into concentrations using these calibration curves. Major elements are reported as percent oxides and converted to elemental values using molar masses. Minor elements are expressed in parts per million (ppm). Details about the analyses are presented in Table **T1**.

4. Results

Results for each site are presented in Tables **T2**, **T3**, **T4**, **T5**, **T6**, **T7**, **T8**, and **T9**, respectively.

4.1. Major elements

Major elements are represented as a function of sediment depth for all sites (Figure **F2**, Sites U1545 and U1546; Figure **F3**, Sites U1547 and U1548; Figure **F4**, Sites U1549 and U1552; Figure **F5**, Site U1550; Figure **F6**, Site U1551). Chlorine (Cl) and sodium (Na) are not included in the graphical representations. Overall, averaged concentrations of major elements are very similar at all sites, with only small differences in terrestrial markers (aluminum [Al], iron [Fe], and titanium [Ti]) at Sites U1550 and U1551 (Table **T10**), which exhibit slightly higher terrestrial inputs.

When normalized to Al (Figure **F7**), only Fe and potassium (K) are linearly correlated, leading to an Fe/Al ratio of 0.48 and a K/Al ratio of 0.32. Ti is also correlated to Al, although not linearly, denoting a potential enrichment in titanium in some samples. These correlations confirm that these elements are mainly derived from lithogenic sources. Silicon (Si) is not correlated to Al, indeed confirming a mixed source between terrestrial and marine, with a significant input of biogenic silica from diatoms. Magnesium (Mg) seems to be correlated to Al except in ~20 samples that are enriched in Mg, probably due to dolomite formation. The Mg versus calcium (Ca) plot yields a narrow range of Mg concentrations for a wide range of Ca (due to carbonate precipitation), with the same 20 samples reaching higher values of Mg (dolomite formation). Overall, major element concentrations and geochemical ratios toward Al are similar to those reported during DSDP

Leg 64 for Sites 477 to 481 in the same area (Niemitz, 1982), except the DSDP samples exhibit higher variability (Table **T11**).

When compared to the North American shale composite (NASC) (Gromet et al., 1984) and average upper crust (McLennan, 2001) (Table **T11**), the concentrations of Al, Fe, K, manganese (Mn), and Ti are lower in the Guaymas Basin, but their ratios normalized to Al are similar, implying a dilution of terrestrial materials with marine production. This marine production is reflected by the higher Si/Al ratio.

Table T2. XRF data for major and minor elements, Site U1545. **Download table in CSV format.**

Table T3. XRF data for major and minor elements, Site U1546. **Download table in CSV format.**

Table T4. XRF data for major and minor elements, Site U1547. **Download table in CSV format.**

Table T5. XRF data for major and minor elements, Site U1548. **Download table in CSV format.**

Table T6. XRF data for major and minor elements, Site U1549. **Download table in CSV format.**

Table T7. XRF data for major and minor elements, Site U1550. **Download table in CSV format.**

Table T8. XRF data for major and minor elements, Site U1551. **Download table in CSV format.**

Table T9. XRF data for major and minor elements, Site U1552. **Download table in CSV format.**

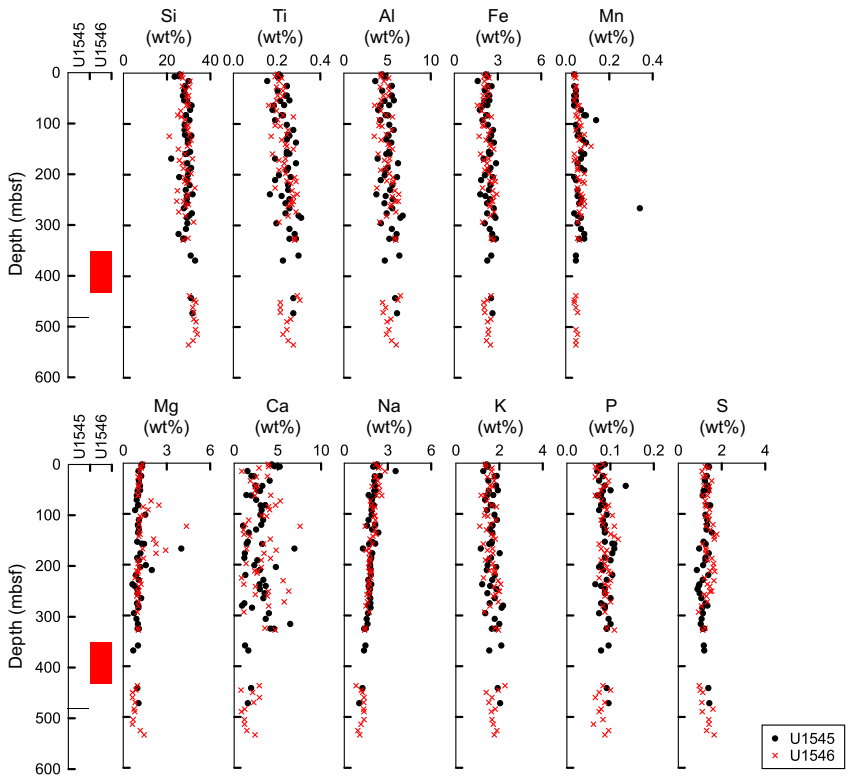

Figure F2. Downcore variation of major element concentrations, Sites U1545 and U1546. Sill recovery is shown in the left column.

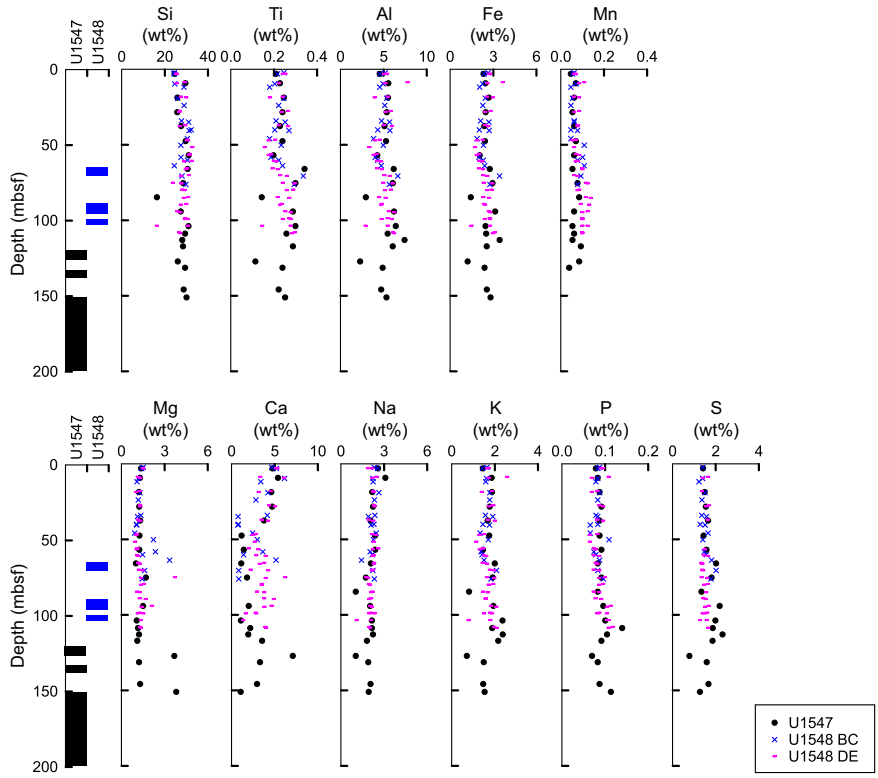

Figure F3. Downcore variation of major element concentrations, Sites U1547 and U1548. Sill recovery is shown in the left column.

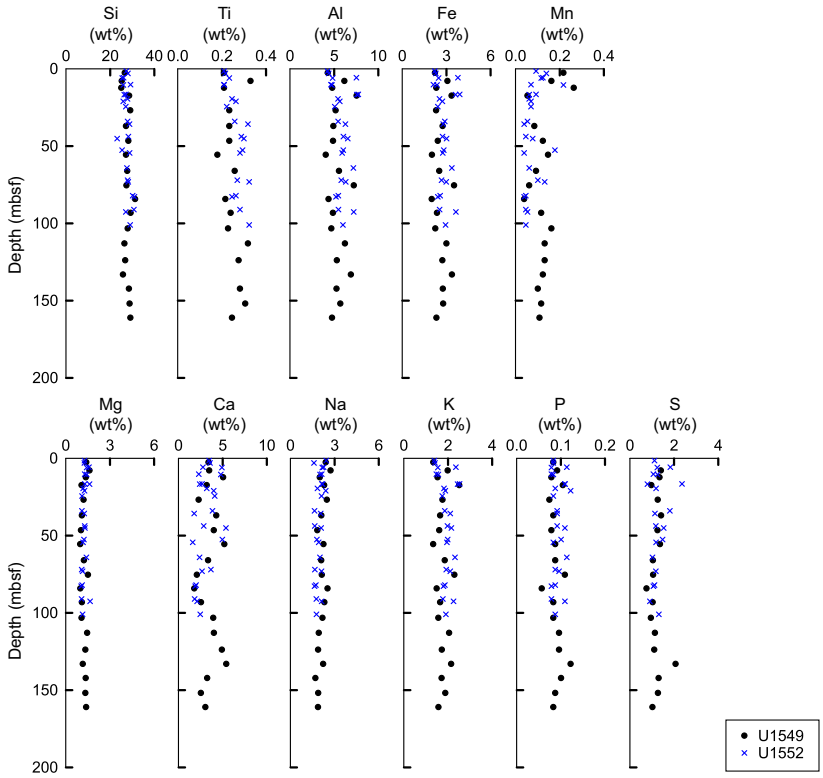

Figure F4. Downcore variation of major element concentrations, Sites U1549 and U1552.

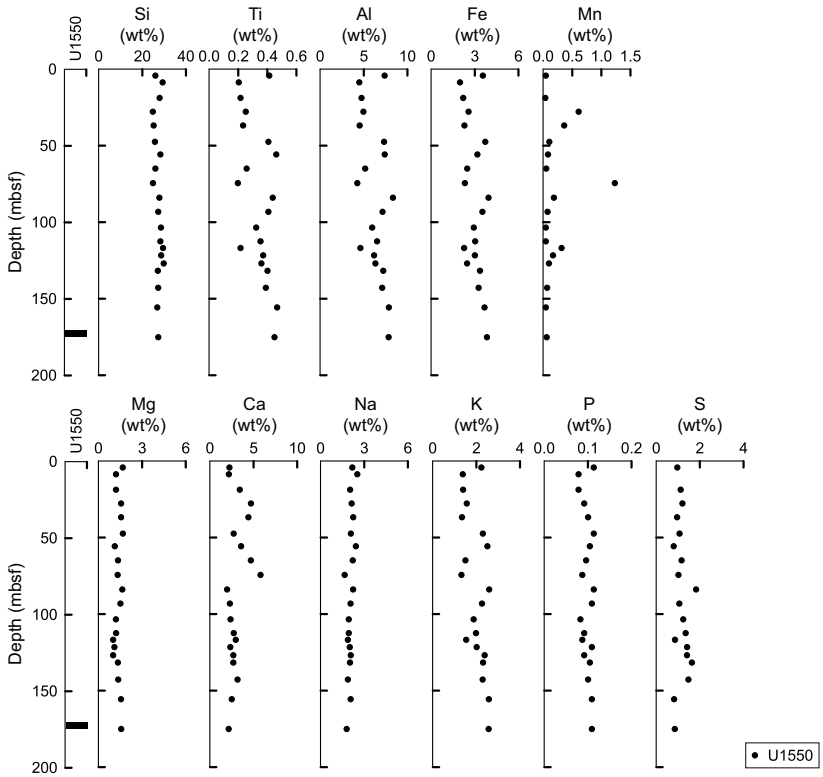

Figure F5. Downcore variation of major element concentrations, Site U1550. Sill recovery is shown in the left column.

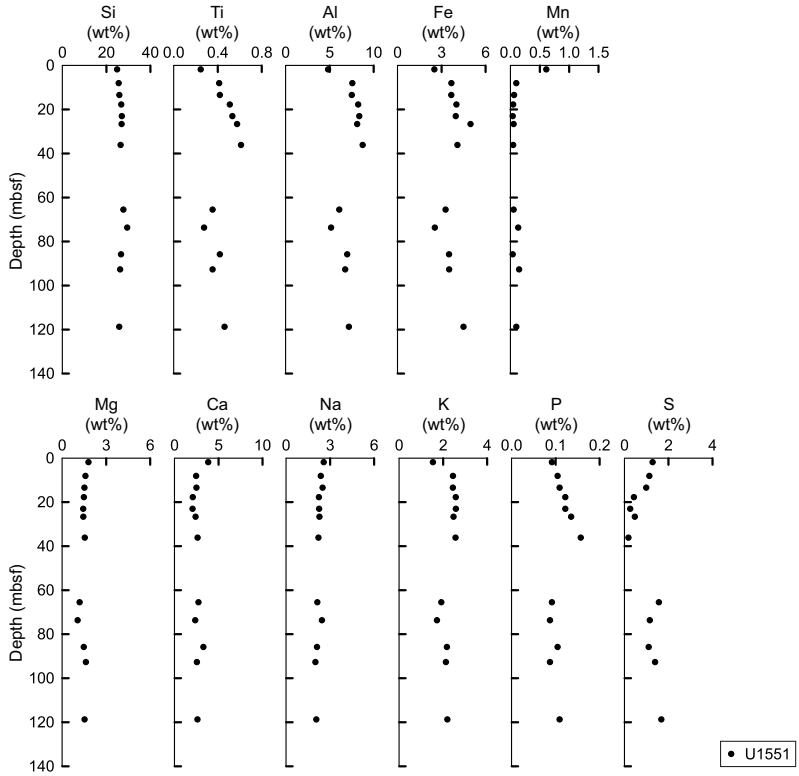

Figure F6. Downcore variation of major element concentrations, Site U1551.

4.2. Minor elements

When the mass of sediment available was not sufficient for pressed pellets, minor elements were not measured (NM); when it was available, they were measured on fused beads (Tables **T2**, **T3**, **T4**, **T5**, **T6**, **T7**, **T8**, **T9**). Minor/trace elements are represented as a function of sediment depth for all sites (Figure **F8**, Sites U1545 and U1546; Figure **F9**, Sites U1547 and U1548; Figure **F10**, Sites U1549 and U1552; Figure **F11**, Site U1550; Figure **F12**, Site U1551).

Except for a few values close to the detection limit, arsenic (As), lead (Pb), and scandium (Sc) concentrations remain below the detection limit (20 ppm) at all sites and are thus not present in tables or illustrations.

Barium (Ba) is associated with various particulate phases in marine sediments (e.g., organic matter, carbonates, opal, ferromanganese oxyhydroxides, detrital material, and barite). It is commonly used as a proxy for (paleo)productivity. The general trend in Ba varies downcore between 400 and 800 ppm, with maxima at Sites U1548, U1549, and U1550 (Figures **F9**, **F10**, **F11**). The average value through all sites is similar to the average of the upper crust and in the same range as the NASC (Table **T12**).

Bromine (Br) in the particulate phase of sediments is thought to be associated with organic matter (Harvey, 1980), and the Br to organic carbon (Br/OC) ratio has been used as a source indicator for organic matter (e.g., Mayer et al., 1981). That explains the large variations observed in Br concentrations along sedimentary cores (Figures **F8**, **F9**, **F10**, **F11**, **F12**) and between sites (Table **T13**), which are also recorded in the OC contents (**Teske et al.**, 2021c; **Teske et al.**, 2021d; **Teske et al.**,

Table T10. Average concentrations of major elements, Expedition 385. **Download table in CSV format.**

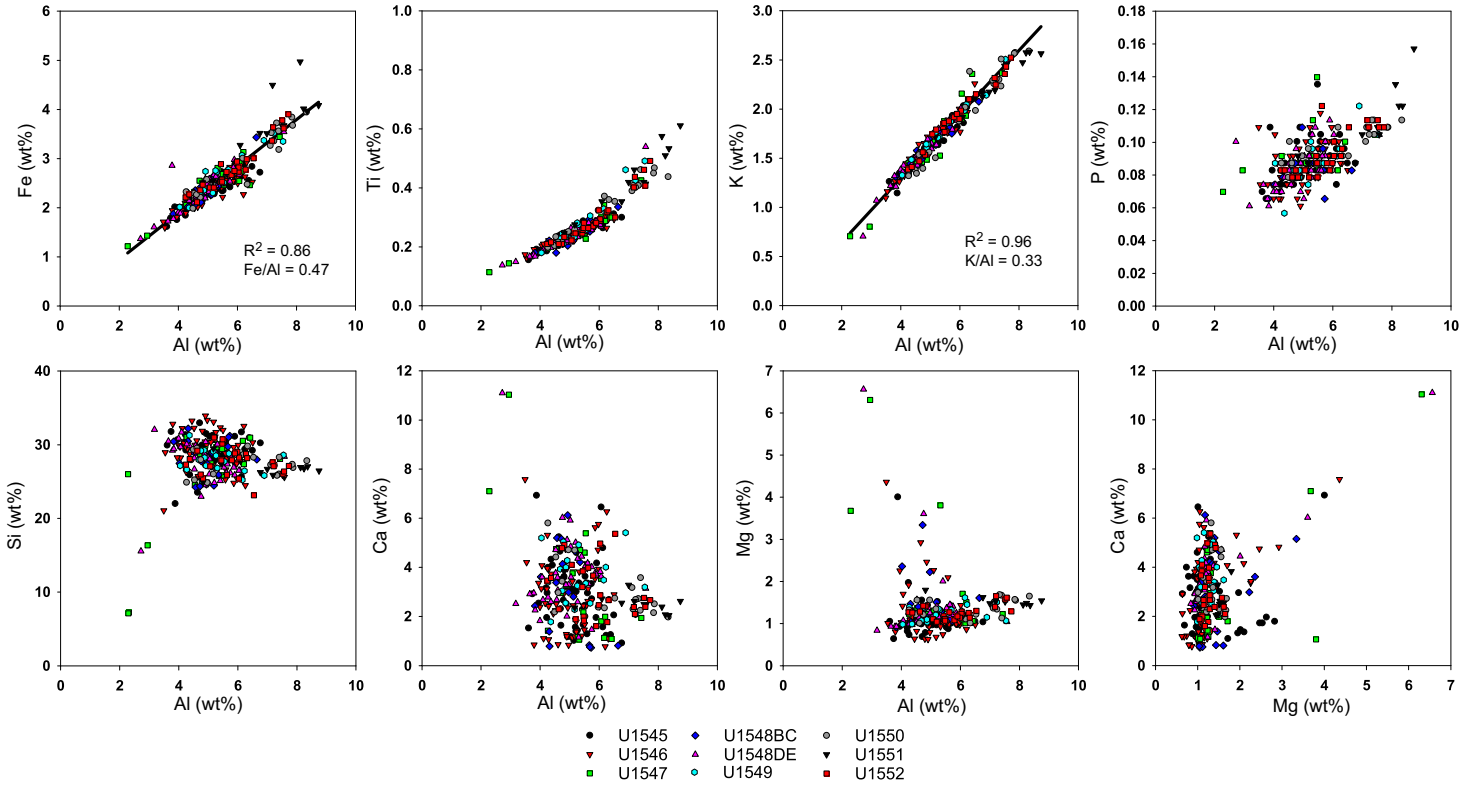

Figure F7. Biplots of selected major elements (Fe, Ti, K, P, Si, Ca, and Mg) normalized to Al and Ca normalized to Mg, Expedition 385.

Table T11. Average major element concentration and ratios for Expedition 385 compared to sediments from the Guaymas Basin (DSDP Leg 64 Sites 477–481), NASC, and average upper crust. **Download table in CSV format.**

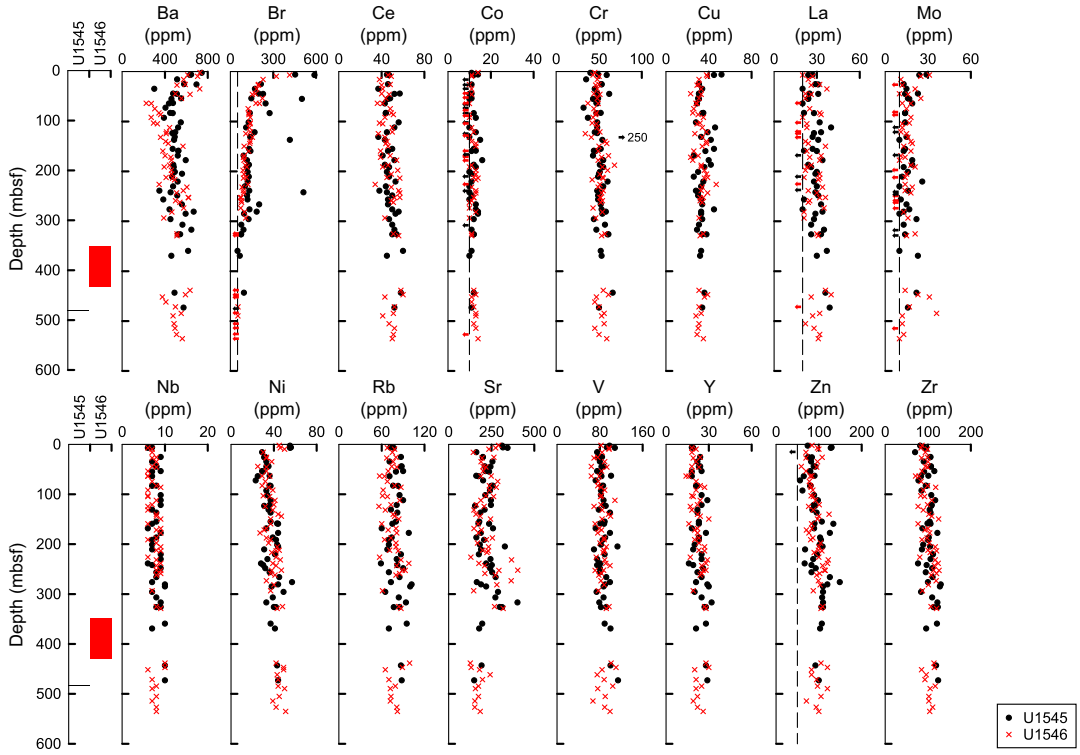

Figure F8. Downcore variation of minor element concentrations, Sites U1545 and U1546. Sill recovery is shown in the left column. Dashed lines represent detection limit, and arrows point to values below this detection limit.

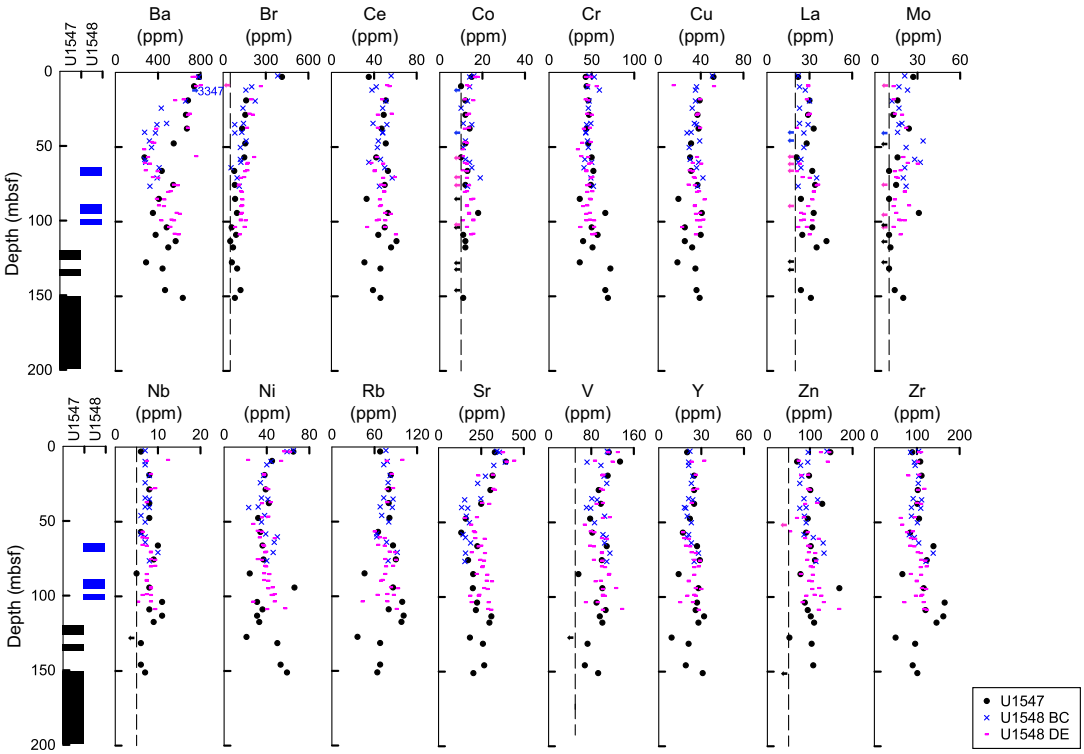

Figure F9. Downcore variation of minor element concentrations, Sites U1547 and U1548. Sill recovery is shown in the left column. Dashed lines represent detection limit, and arrows point to values below this detection limit.

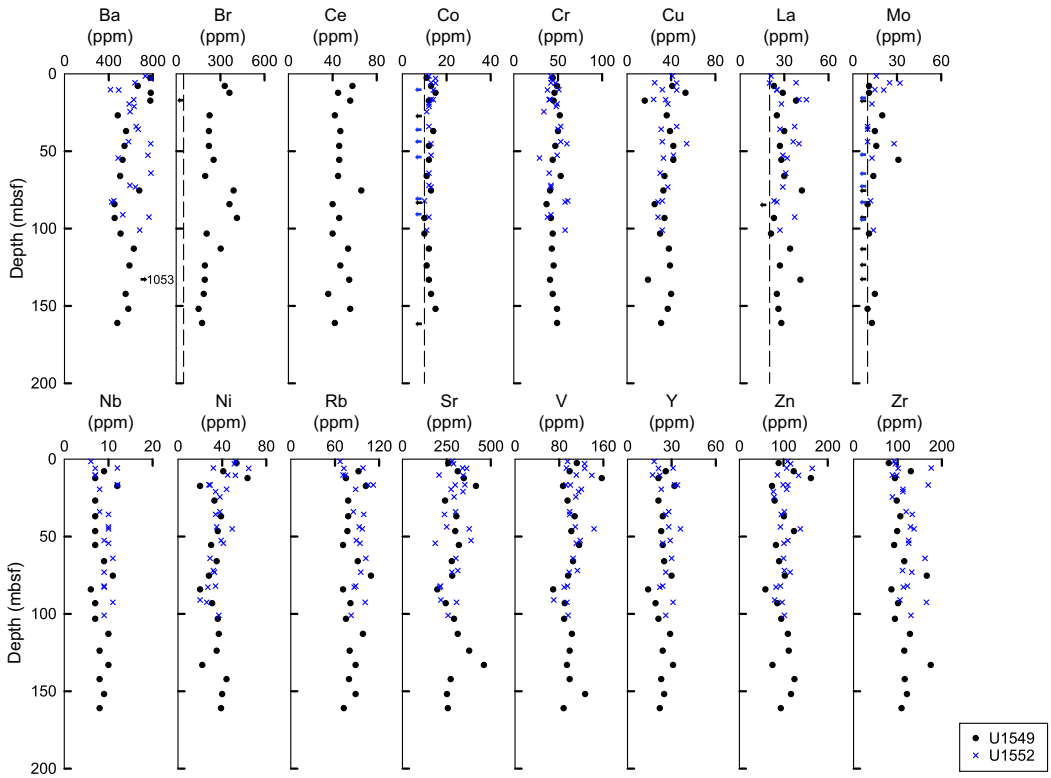

Figure F10. Downcore variation of minor element concentrations, Sites U1549 and U1552. Dashed lines represent detection limit, and arrows point to values below this detection limit.

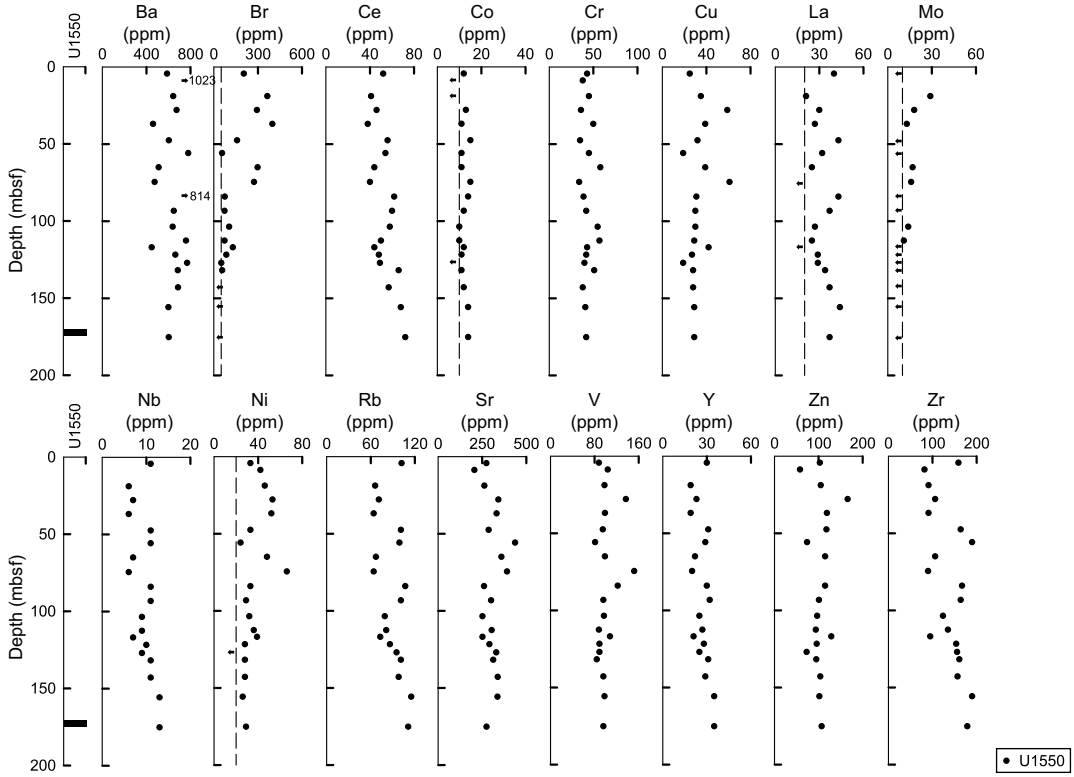

Figure F11. Downcore variation of minor element concentrations, Site U1550. Sill recovery is shown in the left column. Dashed lines represent detection limit, and arrows point to values below this detection limit.

2021e; **Teske et al.**, 2021f; **Teske et al.**, 2021g; **Teske et al.**, 2021h; **Teske et al.**, 2021i). It also explains the much higher values in the organic-rich Guaymas Basin sediments compared with the NASC and average upper crust (Table **T13**).

Cerium (Ce) and lanthanum (La) are light rare earth elements, and their anomalies can be used to highlight specific processes (e.g., oxidative scavenging of Ce by Fe and Mn hydroxides; Bau and Koschinsky, 2009). They exhibit similar averaged values among sites, around 47 ppm for Ce and 28 ppm for La, except at Sites U1550 and U1551 where averages are slightly higher (53 and 62 ppm for Ce and 33 and 39 for La, respectively; Table **T13**). The Ce averaged value in the Guaymas Basin is lower compared to the NASC or the average upper crust (48 vs. 64–67 ppm), whereas the La averaged value is similar (29 vs. 30–31 ppm) (Table **T12**).

Of the other transition metals, cobalt (Co), chromium (Cr), copper (Cu), molybdenum (Mo), niobium (Nb), nickel (Ni), rubidium (Ru), vanadium (V), and yttrium (Y) do not exhibit sharp differences between sites (Table **T13**). However, they are significantly different from the NASC values or the average upper crust when data are available (Table **T12**).

Strontium (Sr) is fixed by calcifying organisms at the same time as Ca and is thus a marker for biogenic origin. It is used to discriminate types of carbonate rocks because it is preferentially incorporated into aragonite. The average values vary throughout sites from a minima of 216 ± 60 ppm at Site U1546 to a maxima of 329 ± 50 ppm at Site U1551 (Table **T13**). The global average lies somewhere between the NASC and the average upper crust value (Table **T12**).

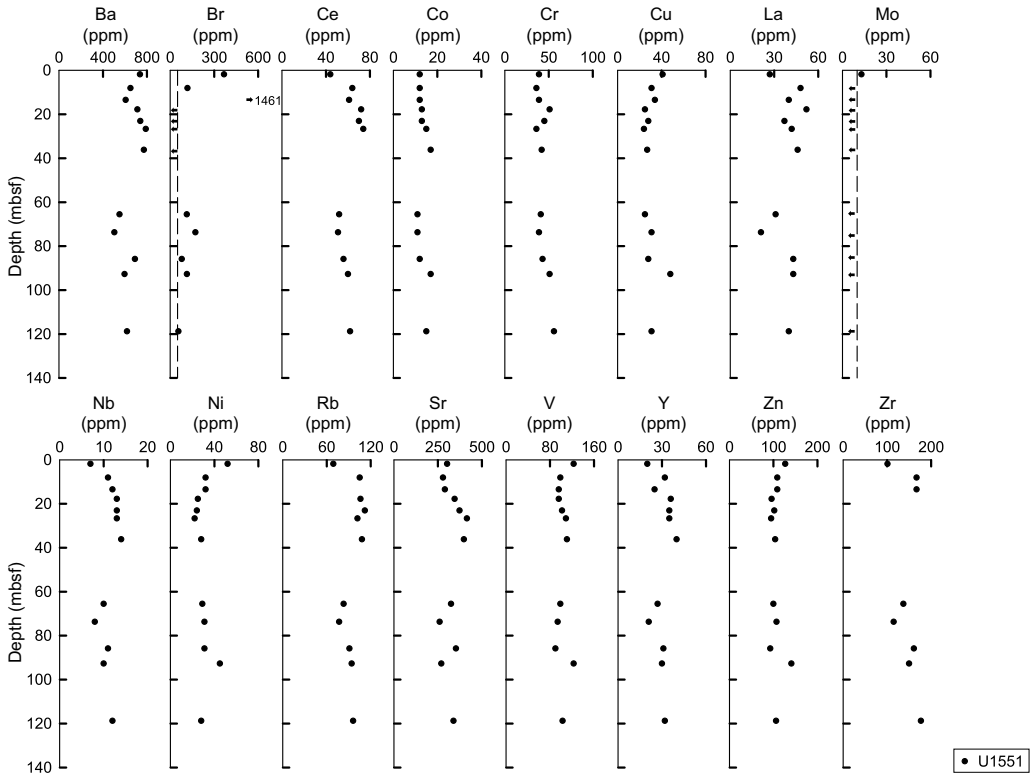

Figure F12. Downcore variation of minor element concentrations, Site U1551. Dashed lines represent detection limit, and arrows point to values below this detection limit.

Table T12. Average concentrations of minor/trace elements, Expedition 385. **Download table in CSV format.**

Table T13. Average minor/trace element concentration from Expedition 385 samples compared to sediments from the Guaymas Basin (DSDP Leg 64 Sites 477–481), NASC, and average upper crust. **Download table in CSV format.**

Zinc (Zn) concentrations remain low (<200 ppm) at all sites (Table **T13**), and the global average is in the same range as the average upper crust (Table **T12**). The global average calculated in this study is much lower than the one found in nearby sites drilled during DSDP Leg 64 (99 vs. 228 ppm; Table **T12**) and could be evidence for the lack of visible influence of the fluids in the Expedition 385 cores.

Zirconium (Zr) can be used in the determination of ash layers. The averaged values at all sites range from 101 ± 14 at Site U1546 to 169 ± 40 ppm at Site U1551. The global averaged value is lower than the average upper crust (111 vs. 190 ppm; Table **T12**).

5. Acknowledgments

This research used samples provided by the International Ocean Discovery Program (IODP), which is sponsored by the US National Science Foundation and participating countries. We acknowledge the outstanding efforts of the drilling personnel and Science Party for IODP Expedition 385. We also thank Armelle Riboulleau, Myriam Kars, and Ivano Aiello for constructive discussion about these data and Mark Zindorf for reviewing this data report. This work was funded by IFREMER and the French National Center for Scientific Research (CNRS) through a postcruise grant from IODP France.

References

Bau, M., and Koschinsky, A., 2009. Oxidative scavenging of cerium on hydrous Fe oxide: evidence from the distribution of rare earth elements and yttrium between Fe oxides and Mn oxides in hydrogenetic ferromanganese crusts. Geochemical Journal, 43(1):37–47. **https://doi.org/10.2343/geochemj.1.0005**

Calvert, S.E., 1966. Accumulation of diatomaceous silica in the sediments of the Gulf of California. Geological Society of America Bulletin, 77(6):569–596. **https://doi.org/10.1130/0016-7606(1966)77[569:AODSIT]2.0.CO;2**

Einsele, G., Gieskes, J.M., Curray, J., Moore, D.M., Aguayo, E., Aubry, M.-P., Fornari, D., Guerrero, J., Kastner, M., Kelts, K., Lyle, M., Matoba, Y., Molina-Cruz, A., Niemitz, J., Rueda, J., Saunders, A., Schrader, H., Simoneit, B., and Vacquier, V., 1980. Intrusion of basaltic sills into highly porous sediments, and resulting hydrothermal activity. Nature, 283(5746):441–445. **https://doi.org/10.1038/283441a0**

Gromet, L.P., Haskin, L.A., Korotev, R.L., and Dymek, R.F., 1984. The "North American shale composite": its compilation, major and trace element characteristics. Geochimica et Cosmochimica Acta, 48(12):2469–2482. **https://doi.org/10.1016/0016-7037(84)90298-9**

Harvey, G.R., 1980. A study of the chemistry of iodine and bromine in marine sediments. Marine Chemistry, 8(4):327–332. **https://doi.org/10.1016/0304-4203(80)90021-3**

Mayer, L.M., Macko, S.A., Mook, W.H., and Murray, S., 1981. The distribution of bromine in coastal sediments and its use as a source indicator for organic matter. Organic Geochemistry, 3(1):37–42. **https://doi.org/10.1016/0146-6380(81)90011-5**

McLennan, S.M., 2001. Relationships between the trace element composition of sedimentary rocks and upper continental crust. Geochemistry, Geophysics, Geosystems, 2(4):2000GC000109. **https://doi.org/10.1029/2000GC000109**

Niemitz, J.W., 1982. Geochemistry of sediments, Leg 64, Gulf of California. In Curray, J.R., Moore, D.G., et al., Initial Reports of the Deep Sea Drilling Project. 64: Washington, DC (US Government Printing Office), 695–713. **https://doi.org/10.2973/dsdp.proc.64.117.1982**

Sturz, A.A., Sturdivant, A.E., Leif, R.N., Simoneit, B.R.T., and Gieskes, J.M., 1996. Evidence for retrograde hydrothermal reactions in near surface sediments of Guaymas Basin, Gulf of California. Applied Geochemistry, 11(5):645–665. **https://doi.org/10.1016/S0883-2927(96)00031-5**

Teske, A., Lizarralde, D., Höfig, T.W., Aiello, I.W., Ash, J.L., Bojanova, D.P., Buatier, M.D., Edgcomb, V.P., Galerne, C.Y., Gontharet, S., Heuer, V.B., Jiang, S., Kars, M.A.C., Khogenkumar Singh, S., Kim, J.-H., Koornneef, L.M.T., Marsaglia, K.M., Meyer, N.R., Morono, Y., Negrete-Aranda, R., Neumann, F., Pastor, L.C., Peña-Salinas, M.E., Pérez Cruz, L.L., Ran, L., Riboulleau, A., Sarao, J.A., Schubert, F., Stock, J.M., Toffin, L.M.A.A., Xie, W., Yamanaka, T., and Zhuang, G., 2021a. Expedition 385 methods. In Teske, A., Lizarralde, D., Höfig, T.W., and the Expedition 385 Scientists, Guaymas Basin Tectonics and Biosphere. Proceedings of the International Ocean Discovery Program, 385: College Station, TX (International Ocean Discovery Program). **https://doi.org/10.14379/iodp.proc.385.102.2021**

Teske, A., Lizarralde, D., Höfig, T.W., Aiello, I.W., Ash, J.L., Bojanova, D.P., Buatier, M.D., Edgcomb, V.P., Galerne, C.Y., Gontharet, S., Heuer, V.B., Jiang, S., Kars, M.A.C., Khogenkumar Singh, S., Kim, J.-H., Koornneef, L.M.T., Marsaglia, K.M., Meyer, N.R., Morono, Y., Negrete-Aranda, R., Neumann, F., Pastor, L.C., Peña-Salinas, M.E., Pérez Cruz, L.L., Ran, L., Riboulleau, A., Sarao, J.A., Schubert, F., Stock, J.M., Toffin, L.M.A.A., Xie, W., Yamanaka, T., and Zhuang, G., 2021b. Expedition 385 summary. In Teske, A., Lizarralde, D., Höfig, T.W., and the Expedition 385 Scientists, Guaymas Basin Tectonics and Biosphere. Proceedings of the International Ocean Discovery Program,

385: College Station, TX (International Ocean Discovery Program). **https://doi.org/10.14379/iodp.proc.385.101.2021**

Teske, A., Lizarralde, D., Höfig, T.W., Aiello, I.W., Ash, J.L., Bojanova, D.P., Buatier, M.D., Edgcomb, V.P., Galerne, C.Y., Gontharet, S., Heuer, V.B., Jiang, S., Kars, M.A.C., Khogenkumar Singh, S., Kim, J.-H., Koornneef, L.M.T., Marsaglia, K.M., Meyer, N.R., Morono, Y., Negrete-Aranda, R., Neumann, F., Pastor, L.C., Peña-Salinas, M.E., Pérez Cruz, L.L., Ran, L., Riboulleau, A., Sarao, J.A., Schubert, F., Stock, J.M., Toffin, L.M.A.A., Xie, W., Yamanaka, T., and Zhuang, G., 2021c. Site U1545. In Teske, A., Lizarralde, D., Höfig, T.W., and the Expedition 385 Scientists, Guaymas Basin Tectonics and Biosphere. Proceedings of the International Ocean Discovery Program, 385: College Station, TX (International Ocean Discovery Program). **https://doi.org/10.14379/iodp.proc.385.103.2021**

Teske, A., Lizarralde, D., Höfig, T.W., Aiello, I.W., Ash, J.L., Bojanova, D.P., Buatier, M.D., Edgcomb, V.P., Galerne, C.Y., Gontharet, S., Heuer, V.B., Jiang, S., Kars, M.A.C., Khogenkumar Singh, S., Kim, J.-H., Koornneef, L.M.T., Marsaglia, K.M., Meyer, N.R., Morono, Y., Negrete-Aranda, R., Neumann, F., Pastor, L.C., Peña-Salinas, M.E., Pérez Cruz, L.L., Ran, L., Riboulleau, A., Sarao, J.A., Schubert, F., Stock, J.M., Toffin, L.M.A.A., Xie, W., Yamanaka, T., and Zhuang, G., 2021d. Site U1546. In Teske, A., Lizarralde, D., Höfig, T.W., and the Expedition 385 Scientists, Guaymas Basin Tectonics and Biosphere. Proceedings of the International Ocean Discovery Program, 385: College Station, TX (International Ocean Discovery Program). **https://doi.org/10.14379/iodp.proc.385.104.2021**

Teske, A., Lizarralde, D., Höfig, T.W., Aiello, I.W., Ash, J.L., Bojanova, D.P., Buatier, M.D., Edgcomb, V.P., Galerne, C.Y., Gontharet, S., Heuer, V.B., Jiang, S., Kars, M.A.C., Khogenkumar Singh, S., Kim, J.-H., Koornneef, L.M.T., Marsaglia, K.M., Meyer, N.R., Morono, Y., Negrete-Aranda, R., Neumann, F., Pastor, L.C., Peña-Salinas, M.E., Pérez Cruz, L.L., Ran, L., Riboulleau, A., Sarao, J.A., Schubert, F., Stock, J.M., Toffin, L.M.A.A., Xie, W., Yamanaka, T., and Zhuang, G., 2021e. Sites U1547 and U1548. In Teske, A., Lizarralde, D., Höfig, T.W., and the Expedition 385 Scientists, Guaymas Basin Tectonics and Biosphere. Proceedings of the International Ocean Discovery Program, 385: College Station, TX (International Ocean Discovery Program). **https://doi.org/10.14379/iodp.proc.385.105.2021**

Teske, A., Lizarralde, D., Höfig, T.W., Aiello, I.W., Ash, J.L., Bojanova, D.P., Buatier, M.D., Edgcomb, V.P., Galerne, C.Y., Gontharet, S., Heuer, V.B., Jiang, S., Kars, M.A.C., Khogenkumar Singh, S., Kim, J.-H., Koornneef, L.M.T., Marsaglia, K.M., Meyer, N.R., Morono, Y., Negrete-Aranda, R., Neumann, F., Pastor, L.C., Peña-Salinas, M.E., Pérez Cruz, L.L., Ran, L., Riboulleau, A., Sarao, J.A., Schubert, F., Stock, J.M., Toffin, L.M.A.A., Xie, W., Yamanaka, T., and Zhuang, G., 2021f. Site U1549. In Teske, A., Lizarralde, D., Höfig, T.W., and the Expedition 385 Scientists, Guaymas Basin Tectonics and Biosphere. Proceedings of the International Ocean Discovery Program, 385: College Station, TX (International Ocean Discovery Program). **https://doi.org/10.14379/iodp.proc.385.106.2021**

Teske, A., Lizarralde, D., Höfig, T.W., Aiello, I.W., Ash, J.L., Bojanova, D.P., Buatier, M.D., Edgcomb, V.P., Galerne, C.Y., Gontharet, S., Heuer, V.B., Jiang, S., Kars, M.A.C., Khogenkumar Singh, S., Kim, J.-H., Koornneef, L.M.T., Marsaglia, K.M., Meyer, N.R., Morono, Y., Negrete-Aranda, R., Neumann, F., Pastor, L.C., Peña-Salinas, M.E., Pérez Cruz, L.L., Ran, L., Riboulleau, A., Sarao, J.A., Schubert, F., Stock, J.M., Toffin, L.M.A.A., Xie, W., Yamanaka, T., and Zhuang, G., 2021g. Site U1550. In Teske, A., Lizarralde, D., Höfig, T.W., and the Expedition 385 Scientists, Guaymas Basin Tectonics and Biosphere. Proceedings of the International Ocean Discovery Program, 385: College Station, TX (International Ocean Discovery Program). **https://doi.org/10.14379/iodp.proc.385.107.2021**

Teske, A., Lizarralde, D., Höfig, T.W., Aiello, I.W., Ash, J.L., Bojanova, D.P., Buatier, M.D., Edgcomb, V.P., Galerne, C.Y., Gontharet, S., Heuer, V.B., Jiang, S., Kars, M.A.C., Khogenkumar Singh, S., Kim, J.-H., Koornneef, L.M.T., Marsaglia, K.M., Meyer, N.R., Morono, Y., Negrete-Aranda, R., Neumann, F., Pastor, L.C., Peña-Salinas, M.E., Pérez Cruz, L.L., Ran, L., Riboulleau, A., Sarao, J.A., Schubert, F., Stock, J.M., Toffin, L.M.A.A., Xie, W., Yamanaka, T., and Zhuang, G., 2021h. Site U1551. In Teske, A., Lizarralde, D., Höfig, T.W., and the Expedition 385 Scientists, Guaymas Basin Tectonics and Biosphere. Proceedings of the International Ocean Discovery Program, 385: College Station, TX (International Ocean Discovery Program). **https://doi.org/10.14379/iodp.proc.385.108.2021**

Teske, A., Lizarralde, D., Höfig, T.W., Aiello, I.W., Ash, J.L., Bojanova, D.P., Buatier, M.D., Edgcomb, V.P., Galerne, C.Y., Gontharet, S., Heuer, V.B., Jiang, S., Kars, M.A.C., Khogenkumar Singh, S., Kim, J.-H., Koornneef, L.M.T., Marsaglia, K.M., Meyer, N.R., Morono, Y., Negrete-Aranda, R., Neumann, F., Pastor, L.C., Peña-Salinas, M.E., Pérez Cruz, L.L., Ran, L., Riboulleau, A., Sarao, J.A., Schubert, F., Stock, J.M., Toffin, L.M.A.A., Xie, W., Yamanaka, T., and Zhuang, G., 2021i. Site U1552. In Teske, A., Lizarralde, D., Höfig, T.W., and the Expedition 385 Scientists, Guaymas Basin Tectonics and Biosphere. Proceedings of the International Ocean Discovery Program, 385: College Station, TX (International Ocean Discovery Program). **https://doi.org/10.14379/iodp.proc.385.109.2021**

Teske, A., McKay, L.J., Ravelo, A.C., Aiello, I., Mortera, C., Núñez-Useche, F., Canet, C., Chanton, J.P., Brunner, B., Hensen, C., Ramírez, G.A., Sibert, R.J., Turner, T., White, D., Chambers, C.R., Buckley, A., Joye, S.B., Soule, S.A., and Lizarralde, D., 2019. Characteristics and evolution of sill-driven off-axis hydrothermalism in Guaymas Basin – the Ringvent site. Scientific Reports, 9(1):13847. **https://doi.org/10.1038/s41598-019-50200-5**

Von Damm, K.L., Edmond, J.M., Grant, B., Measures, C.I., Walden, B., and Weiss, R.F., 1985. Chemistry of submarine hydrothermal solutions at 21°N, East Pacific Rise. Geochimica et Cosmochimica Acta, 49(11):2197–2220. **https://doi.org/10.1016/0016-7037(85)90222-4**